Defence Technology 13 (2017) 86–91

Contents lists available at ScienceDirect

Defence Technology

journal homepage: www.elsevier.com/locate/dt

Effect of tool plunge depth on reinforcement particles distribution in surface composite fabrication via friction stir processing

Sandeep Rathee [a, *], Sachin Maheshwari [a], Arshad Noor Siddiquee [b], Manu Srivastava [a]

[a] Division of Manufacturing Processes and Automation Engineering (MPAE), Netaji Subhas Institute of Technology, New Delhi, India
[b] Department of Mechanical Engineering, Jamia Millia Islamia, A Central University, New Delhi, India

ARTICLE INFO

Article history:
Received 31 August 2016
Received in revised form
20 October 2016
Accepted 15 November 2016
Available online 24 December 2016

Keywords:
Metal matrix composites
Friction stir processing
Tool plunge depth
Microstructural characterization

ABSTRACT

Aluminium matrix surface composites are gaining alluring role especially in aerospace, defence, and marine industries. Friction stir processing (FSP) is a promising novel solid state technique for surface composites fabrication. In this study, AA6061/SiC surface composites were fabricated and the effect of tool plunge depth on pattern of reinforcement particles dispersion in metal matrix was investigated. Six varying tool plunge depths were chosen at constant levels of shoulder diameter and tool tilt angle to observe the exclusive effect of plunge variation. Process parameters chosen for the experimentation are speed of rotation, travel speed and tool tilt angle which were taken as 1400 rpm, 40 mm/min, and 2.5°respectively. Macro and the microstructural study were performed using stereo zoom and optical microscope respectively. Results reflected that lower plunge depth levels lead to insufficient heat generation and cavity formation towards the stir zone center. On the other hand, higher levels of plunge depth result in ejection of reinforcement particles and even sticking of material to tool shoulder. Thus, an optimal plunge depth is needed in developing defect free surface composites.

1. Introduction

It is common knowledge that aluminium alloys are materials of choice for various structural applications in aerospace, defence, automobile, and marine industries owing to their lower weight density, higher strength to weight ratio and higher corrosion resistance [1]. However, stiffness and strength of some of these alloys is not adequate for some structural purposes thereby necessitating requirement of suitable reinforcement. Aluminium metal matrix composites (AMMCs) exhibit improved metallurgical, mechanical, and tribological characteristics [1–3]. Metal matrix composites (MMCs) can be synthesized using various techniques like laser technique [4], electron beam irradiation [5], plasma spraying [6], casting [7], mechanical alloying [8], etc. Most of these techniques are based on the principle of liquid phase processing which leads to formation of intermetallic reactions and undesirable phases between base metal (BM) and reinforcement [9,10]. In view of the these shortcomings, employment of a process for composite fabrication which can be conducted below melting points of the matrix material can go a long way to improve and consequently optimize the MMCs design and fabrication issue. Friction stir processing (FSP) offers an excellent choice for development of surface composites (SCs) of metal alloys [11].

FSP is a newly developed solid state processing technique which is a variant of friction stir welding (FSW) process initiated at The Welding Institute (TWI) in 1991 [12]. In its simple operation, a non-consumable rotating tool with an exclusively designed pin and shoulder plummets into a BM plate and is made to traverse in predefined direction to cover up the desired realm. Softening and plasticization of BM occurs owing to frictional heat generation between rotating tool and the workpiece [10,13]. As the tool traverses, the material is forged beneath the shoulder resulting in the processed region. The work on composite fabrication using FSP, was started with the maiden work done by Mishra et al. [11]. In this work, composites with Al 5083 alloy as BM and SiC as reinforcement were fabricated. A maximum microhardness of 173 Hv was achieved using 27 vol % of SiC particles which is almost double of the microhardness of BM (85 Hv). Numerous research studies on composite fabrication are reported since the initial work by Mishra et al. and a number of research projects are still in progress. Initially, FSP was used to modify aluminium alloys but with the passage of time FSP has gained a shining role in developing composites of

* Corresponding author. TRF, MPAE Division, NSIT, New Delhi, 110078, India.
E-mail address: rathee8@gmail.com (S. Rathee).
Peer review under responsibility of China Ordnance Society.

http://dx.doi.org/10.1016/j.dt.2016.11.003

other alloys like magnesium [14], copper [15], titanium [16] and even steel [17].

The addition of hard phase reinforcement particles make MMCs brittle [18]. In many engineering applications, the service life of materials mainly depends on the surface properties of materials. Therefore, SCs are mostly prepared by combining a ductile metallic matrix with hard ceramic reinforcement up to a desired depth. The soundness of SCs apart from other aspects mainly depends on optimal selection of process parameters. Several authors [19–22] investigated the effect of various process parameters in developing SCs. Dolatkhah et al. [19] evaluated the effects of rotational and travel speeds, FSP pass count and size of reinforcement particles in fabrication of Al 5052/SiC composites. They reported that speed of rotation and FSP pass counts have major effect on uniform dispersion of reinforcement particles. Similarly, Zohoor et al. [21] investigated the effects of speed of rotation, FSP pass count and size of reinforcement particles in the fabrication of AA5083/Cu composites. They reported that best powder dispersion was achieved with four FSP pass count. Devaraju et al. [20] reported that speed of rotation and type of reinforcement particles have a strong impact on wear, microhardness and tensile strength of fabricated AA 6061/SiC + Al_2O_3 hybrid SCs. Reddy et al. [23] investigated the effect of reinforcement particles (B_4C and SiC) on the wear and mechanical properties of fabricated SCs.

Majority of published research mainly focuses on the evaluation of effects of process parameters, namely tool rotation speed, travel speed, FSP pass count and tool dimensions on the surface and mechanical properties of fabricated SCs. Also, reinforcement particle type and its size remains center of research focus. Literature also report that the SCs imperfections can be reduced by accurate prediction of these process parameters. In addition to these process parameters, correct decision on suitable tool plunge depth (TPD) is also essential to achieve defect free and uniformly distributed SCs. Interestingly, TPD is not changed in-situ after the process has started and investigations on effect of TPD over distribution of reinforcement particles in SCs fabrication are very few. Present work investigates the effect of varying TPD on SCs fabrication by keeping all other parameters constant at optimized level. Six levels of TPD from 0.10 mm to 0.35 mm in steps of 0.05 mm were used to investigate and determine the role of plunge depth on material flow, uniformity of powder dispersion and tendency of defect formation. Additionally, proper care has also been taken to minimize the adverse effects originating from factors like machine vibrations, non-uniformity of BM and backing plate thickness which is normally not paid enough attention.

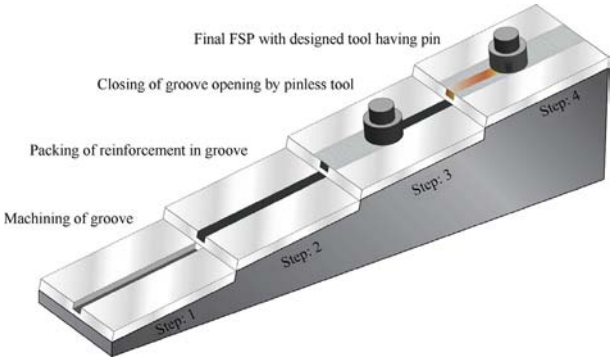

Fig. 2. Steps in SCs fabrication using groove technique.

2. Materials and methods

In this study, AA 6061-T6 alloy sheet of 5 mm thickness was used as base material. AA 6061-T6 is commonly used in aerospace, defence and marine sectors due to its light weight, good strength to weight ratio and good corrosion resistance [24,25]. The composition (weight %) of BM is 0.85% Mg, 0.68% Si, 0.22% Cu, 0.07% Zn, 0.05% Ti, 0.032% Mn, 0.06% Cr and remaining aluminium. FSP samples of size 60 mm wide and 200 mm long were machined from the sheet. SiC powder having average particle size of ~10 μm was used as reinforcement (SEM image is shown in Fig. 1(a). Six such FSP samples were prepared by cleaning them with acetone and machining square grooves of 2 mm width and 2 mm depth along the length. Subsequently, SiC powder was filled and compressed in the groove and upper surface (open) of the groove was closed by means of a tool (15 mm shoulder diameter, see Fig. 1(b) without a pin in order to prevent the sputtering of powder during FSP. Finally, FSP was performed on a retrofitted vertical milling machine as shown in Fig. 3 using a tool with a threaded cylindrical pin. The tools utilized for FSP were made of H-13 tool steel (see Fig. 1(b)). Steps involved in SCs formation using groove technique are schematically illustrated in Fig. 2. The values of process parameters such as speed of rotation, traverse speed and tilt angle of tool (see Table 1) were chosen by trial experiments performed on AA6061

Fig. 1. Showing images of SiC powder and tools used; (a) SEM image of SiC powder; (b) Tools used during FSP.

Fig. 3. FSP setup.

Table 1
Showing constant process parameters used in SCs fabrication.

Sr. No.	Process parameters	Values
1.	Speed of rotation/rpm	1400
2.	Traverse speed/(mm·min^{-1})	40
3.	Tool tilt angle/(°)	2.5
4.	Tool shoulder diameter/mm	20
5.	Tool pin diameter/mm	06
6.	Tool pin length/mm	2.8
7.	Tool pin profile	Threaded

with TPD of 0.20 mm. Six experiments were performed by varying TPD from 0.10 mm to 0.35 mm in steps of 0.05 mm and keeping all other parameters (as shown in Table 1) as constant.

After single pass FSP on all six samples, coupons for macro and microstructural study were machined using wire-EDM from the middle of each SC sample in a direction perpendicular to the processing route. These samples were polished following standard metallographic procedures and then etched with Keller's reagent (175 ml water, 20 ml HNO_3, 3 ml HCL and 2 ml HF) for 30 s. Macrographic images were taken by stereo zoom microscope while micrographic images were taken by metallurgical optical microscope and scanning electron microscope.

3. Results

3.1. Macroscopic observations

Table 2 shows macroscopic images of SCs (S_1-S_6) along with their visual description. It is evident from the macrographic images that the pattern of reinforcement particles distribution in of all SCs is different. The width of processed region was found to be approximately same as diameter of tool shoulder. However, width/area of stir zone and SC layer depth varies in all SCs.

Table 2
Macroscopic images of all samples (S_1-S_6) along with their description.

Specimen	Macroscopic Image	Description/Visual Observation
Sample 1 (S_1), TPD-0.10 mm		• Large cavity at center of stir zone (SZ) • Shoulder driven flow
Sample 2 (S_2), TPD-0.15 mm	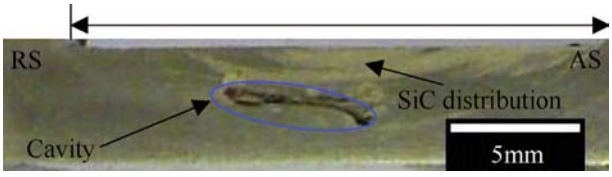	• Powder dispersion increases • Cavity still appears
Sample 3 (S_3), TPD-0.20 mm	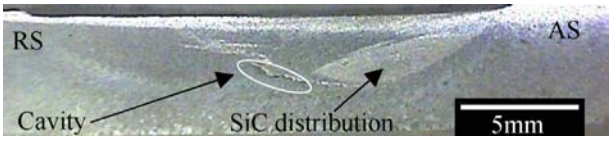	• Cavity size decreases • Powder accumulates in AS
Sample 4 (S_4), TPD-0.25 mm		• Defect free SC • Uniform powder distribution
Sample 5 (S_5), TPD-0.30 mm		• Powder dispersion decreases' • Shoulder driven flow
Sample 6 (S_6), TPD-0.35 mm		• Defect appears • Shoulder driven flow in AS

* AS- advancing side; RS- retreating side.

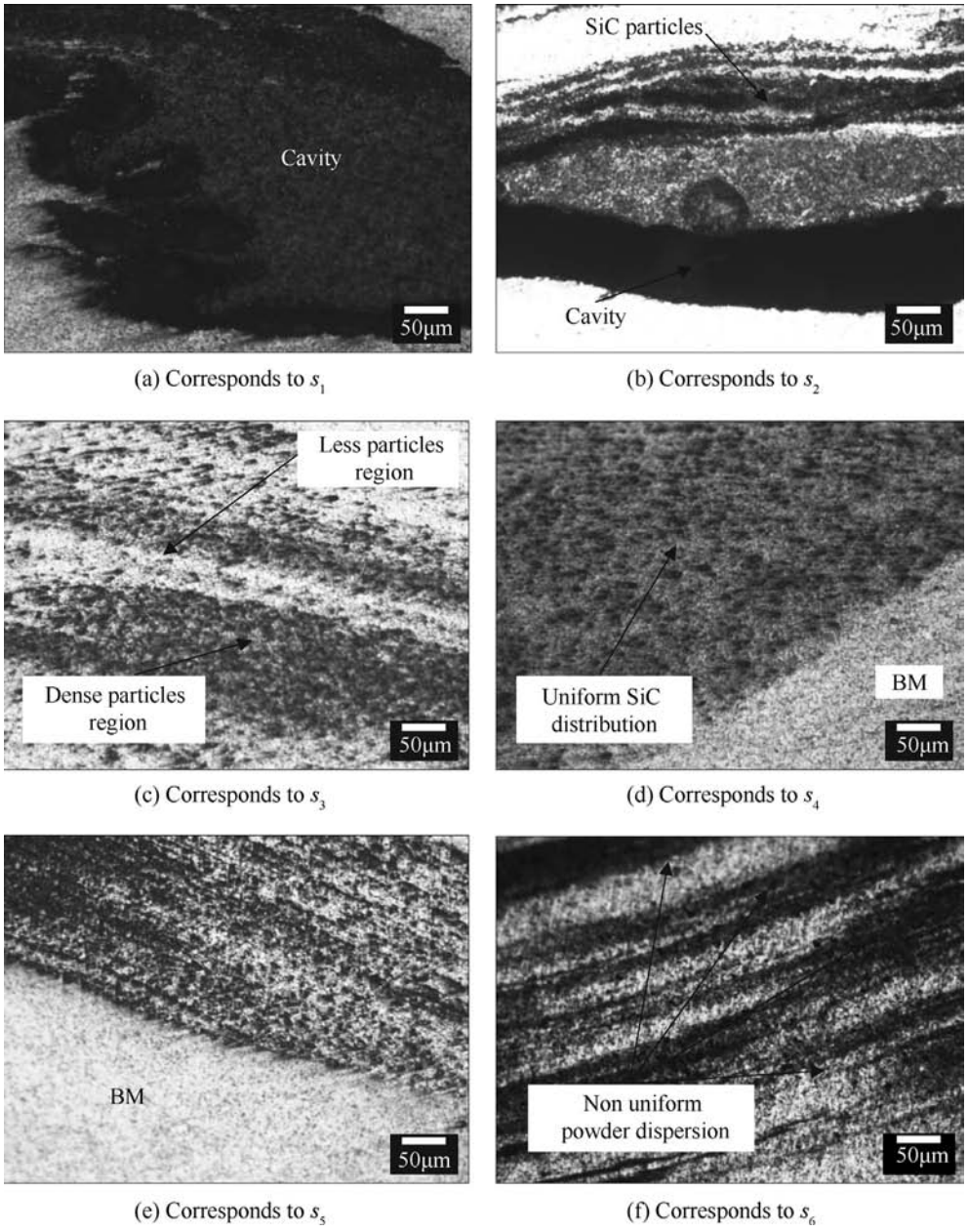

Fig. 4. Showing microstructural images of SCs taken at 100 magnifications, (a) corresponds to S_1; (b) S_2; (c) S_3; (d) S_4; (e) S_5; (f) S_6.

3.2. Microstructural characterization

Fig. 4 (a)-(f) reveals the microstructural images of SCs (S_1-S_6 respectively). A large cavity is present in centre of the SZ (see Fig. 4(a)), which is also visible in macrograph corresponds to S_1. Fig. 4(b) shows that SiC particles dispersion slightly increases and cavity size decreases (with increase in TPD from 0.10 to 0.15 mm) which indicate the improvement in material flow and particles dispersion. With further increase in TPD from 0.15 to 0.20 mm, the improvement in material flow can be further seen in Fig. 4(c) in which more particles were distributed in the aluminium matrix as compared to S_1 and S_2. Finally, uniform dispersion of SiC particles was achieved (at TPD of 0.25 mm) without any defect formation as shown in Fig. 4(d) whose SEM images are shown in Fig. 5. Fig. 4 (e) and (f) shows that the uniformity of powder dispersion decreases (at TPD of 0.30 and 0.35 respectively). Also, the tendency of defect formation increases.

4. Discussion

Image corresponds to S_1 (Table 2) is the macroscopic image of SC fabricated at plunge depth of 0.10 mm. A large cavity defect appears at the center of SZ and powder distribution is very less. Shoulder driven flow causes the powder distribution. SC layer depth is quite less. This may be attributed to less material flow due to low heat generation at lower plunge depth of 0.10 mm. At low plunge depth, the contact area between tool shoulder and base metal is less. With the increase of plunge depth from 0.10 mm to 0.15 mm, the contact area between shoulder and workpiece increases which results in more heat generation. Also, the vertical pressure on the base metal increases resulting in better forging and improved material flow and particles dispersion [26] as shown in S_2 (Table 2). Depth of SC layer also increases. However, a cavity remains unfilled in this sample that implies that heat generation was still not adequate. As plunge depth further increases from 0.15 to 0.20 mm, cavity size

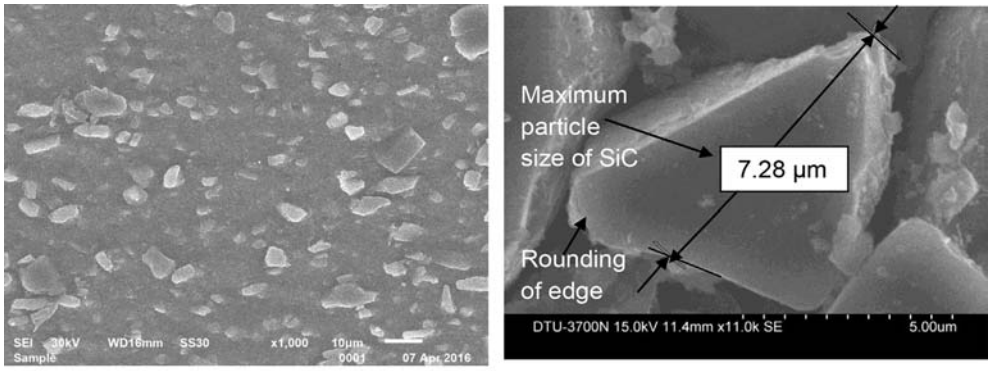

(a) Distribution of SiC particles (b) Maximum particle size of SiC after FSP

Fig. 5. shows the SEM images of SCs fabricated at 0.25 mm plunge depth, (a) distribution of SiC particles; (b) Maximum size of SiC particle after FSP.

decreases to its minimum and uniformity in powder dispersion increases as shown in S_3 (Table 2) and Fig. 4(c). Also, the SC layer achieves a depth which is approximately equal to tool pin height in bulk matrix.

The cavity finally disappears in S_4 (Table 2) fabricated at plunge depth of 0.25 mm owing to sufficient heat generation due to the adequate contact area of tool shoulder and workpiece. Distribution of reinforcement particles also becomes visibly uniform (see Fig. 4(d)). And SC layer depth becomes equal to tool pin height.

Any further increase of TPD from 0.25 to 0.30 and 0.35 mm results in a reduction of powder dispersion and decrease of SC depth as shown in S_5 and S_6 (Table 2) and Fig. 4(e) and (f) respectively. It may be assumed that after an optimum value of TPD, the increase of plunge depth causes excess heat generation which results in more softening of material near tool matrix interface. This excess softening of material leads to more flash generation. The high tool pressure (at higher TPD), the shoulder expels the reinforcement particles with or in form of flash resulting in less dispersion of SiC in the metal matrix. Same results can be seen from S6, in which SiC distribution further decreases and defect appears in the SZ. Also, the frictional mode between shoulder and material (to be stirred) changes from sliding to sticking due to high pressure exerted by tool shoulder. This high pressure can results in thinning and may even damage of specimen. Thus, low penetration depths causes less material flow while high penetration depths results in excessive flash and damage of the specimen.

Fig. 5(a)-(b) shows SEM images of SC fabricated at 0.25 mm plunge depth. It is evident from the figure that SiC particles are well distributed in aluminium matrix and their particle size viz-a-viz original size has reduced drastically. This reduction may occur due to the fragmentation of SiC particles owing to high strain induced by FSP and vigorous stirring action of tool. The vigorous stirring of tool might also have ground the sharp edges of SiC particles (see Fig. 5(b)).

Thus, reduction in the size of SiC particles can be attributed to severe stresses and shear effects caused by the tool rotation. Similar results were reported by other researchers [27,28]. Moreover, the distributed particles have large size variations and maximium size of SiC particles after FSP was found as 7.28 μm (see Fig. 5(b)). The average SiC particle size was found as ~2.1 μm which is a huge reduction as compared to as-received 10 μm average particle size.

This investigation has demonstrated that the size of SiC particles was subdivided during FSP causing an increase in particle density and reduction in grain size and interparticle spacing. Moreover, the scope of FSP for SCs fabrication may be further investigated by using smaller particles size of order of nanometer which may results in further improvement in properties of nano SCs as compared to micro SCs.

5. Conclusions

The practical benefit of this work is to provide adequate TPD to fabricate sound AA 6061/SiC surface composites. Following conclusions are drawn from the present study:

1) Low plunge depth results in less material flow and cavity formation at centre of SZ owing to less heat generation at low contact area between tool shoulder and base metal.
2) The optimum plunge depth obtained from current work is 0.25 mm with 20 mm shoulder diameter and 2.5° tilt angle. The particles were found well distributed in the aluminium matrix.
3) During FSP, fragmentation of SiC particles takes place owing to high plastic strains and stirring action of FSP tool.
4) The penetration depths above the optimum value may results in sticking of workpiece to the shoulder, flashing out of reinforcement particles, thinning of processed specimen and even damage of the specimens.

Acknowledgments

The authors thank the University Grants Commission (UGC) for its financial assistance (vide sanction order No. F.3-40/2012 (SAP-II) under its SAP (DRS-I) sanctioned to the Department of Mechanical Engineering for the project entitled Friction Stir Welding, Ultrasonic Machining.

References

[1] Miracle DB. Metal matrix composites – from science to technological significance. Compos Sci and Technol 2005;65(15–16):2526–40.
[2] Cavaliere P. Mechanical properties of Friction Stir Processed 2618/Al2O3/20p metal matrix composite. Compos Part A Appl Sci Manuf 2005;36(12):1657–65.
[3] Joseph, S., High temperature metal matrix composites for future aerospace systems, in 24th Joint Propulsion Conference 1988, American Institsute of Aeronautics and Astronautics.
[4] Ghosh SK, Saha P. Crack and wear behavior of SiC particulate reinforced aluminium based metal matrix composite fabricated by direct metal laser sintering process. Mater Des 2011;32(1):139–45.
[5] Choo S-H, Lee S, Kwon S-J. Surface hardening of a gray cast iron used for a diesel engine cylinder block using high-energy electron beam irradiation. Metall Mater Trans A 1999;30(5):1211–21.
[6] Xu J, et al. Fabrication and properties of Al2O3–TiB2–TiC/Al metal matrix composite coatings by atmospheric plasma spraying of SHS powders. J Alloys Compd 2016;672:251–9.
[7] Hashim J, Looney L, Hashmi MSJ. Metal matrix composites: production by the stir casting method. J Mater Process Technol 1999;92–93(0):1–7.
[8] Banhart J. Manufacture, characterisation and application of cellular metals and metal foams. Prog Mater Sci 2001;46(6):559–632.

[9] Mishra R.S, Mahoney M.W, Friction stir welding and processing 2007: ASM International.
[10] Mishra RS, Ma ZY. Friction stir welding and processing. Mater Sci Eng R Rep 2005;50(1–2):1–78.
[11] Mishra RS, Ma ZY, Charit I. Friction stir processing: a novel technique for fabrication of surface composite. Mater Sci Eng A 2003;341(1–2):307–10.
[12] Thomas, W.M., TWI, Editor 1991: U.S.
[13] Berbon PB, et al. Friction stir processing: a tool to homogenize nanocomposite aluminum alloys. Scr Mater 2001;44(1):61–6.
[14] Azizieh M, Kokabi AH, Abachi P. Effect of rotational speed and probe profile on microstructure and hardness of AZ31/Al2O3 nanocomposites fabricated by friction stir processing. Mater Des 2011;32(4):2034–41.
[15] Barmouz M, Besharati Givi MK, Seyfi J. On the role of processing parameters in producing Cu/SiC metal matrix composites via friction stir processing: investigating microstructure, microhardness, wear and tensile behavior. Mater Charact 2011;62(1):108–17.
[16] Shamsipur A, Kashani-Bozorg SF, Zarei-Hanzaki A. The effects of friction-stir process parameters on the fabrication of Ti/SiC nano-composite surface layer. Surf Coatings Technol 2011;206(6):1372–81.
[17] Ghasemi-Kahrizsangi A, Kashani-Bozorg SF. Microstructure and mechanical properties of steel/TiC nano-composite surface layer produced by friction stir processing. Surf Coatings Technol 2012;209(0):15–22.
[18] Arora HS, Singh H, Dhindaw BK. Composite fabrication using friction stir processing—a review. Int J Adv Manuf Technol 2012;61(9–12):1043–55.
[19] Dolatkhah A, et al. Investigating effects of process parameters on microstructural and mechanical properties of Al5052/SiC metal matrix composite fabricated via friction stir processing. Mater Des 2012;37(0):458–64.
[20] Devaraju A, et al. Influence of reinforcements (SiC and Al2O3) and rotational speed on wear and mechanical properties of aluminum alloy 6061-T6 based surface hybrid composites produced via friction stir processing. Mater Des 2013;51(0):331–41.
[21] Zohoor M, Besharati Givi MK, Salami P. Effect of processing parameters on fabrication of Al–Mg/Cu composites via friction stir processing. Mater Des 2012;39:358–65.
[22] Sudhakar I, et al. Enhancement of wear and ballistic resistance of armour grade AA7075 aluminium alloy using friction stir processing. Def Technol 2015;11(1):10–7.
[23] Madhusudhan Reddy G, Sambasiva Rao A, Srinivasa Rao K. Friction stir processing for enhancement of wear resistance of ZM21 magnesium alloy. Trans Indian Inst Metals 2013;66(1):13–24.
[24] Devaraju A. K.A., Kotiveerachari B., Influence of rotational speed and reinforcements on wear and mechanical properties of aluminum hybrid composites via friction stir processing. Mater Des 2013;45:576–85.
[25] Mukhopadhyay P. Alloy designation, processing, and Use of AA6XXX series aluminium alloys. ISRN Metall 2012;2012:15.
[26] Asadi P, Faraji G, Besharati M. Producing of AZ91/SiC composite by friction stir processing (FSP). Int J Adv Manuf Technol 2010;51(1–4):247–60.
[27] Salih OS, et al. A review of friction stir welding of aluminium matrix composites. Mater Des 2015;86:61–71.
[28] Palanivel R, et al. Influence of boron nitride nanoparticles on microstructure and wear behavior of AA6082/TiB2 hybrid aluminum composites synthesized by friction stir processing. Mater Des 2016;106:195–204.